Two-Dimensional NMR Studies of Staphylococcal Nuclease. 2. Sequence-Specific Assignments of Carbon-13 and Nitrogen-15 Signals from the Nuclease H124L–Thymidine 3′,5′-Bisphosphate–Ca^{2+} Ternary Complex†

Jinfeng Wang, Andrew P. Hinck, Stewart N. Loh,‡ and John L. Markley*

Department of Biochemistry, College of Agricultural and Life Sciences, University of Wisconsin—Madison, 420 Henry Mall, Madison, Wisconsin 53706

Received June 12, 1989

ABSTRACT: Samples of staphylococcal nuclease H124L (cloned protein overproduced in *Escherichia coli* whose sequence is identical with that of the nuclease isolated from the V8 strain of *Staphylococcus aureus*) were labeled uniformly with carbon-13 (26% ul ^{13}C), uniformly with nitrogen-15 (95% ul ^{15}N), and specifically by incorporating nitrogen-15-labeled leucine ([98% ^{15}N]Leu) or carbon-13-labeled lysine ([26% ul ^{13}C]Lys), arginine ([26% ul ^{13}C]Arg), or methionine ([26% ul ^{13}C]Met). Solutions of the ternary complexes of these analogues (nuclease H124L–pdTp–Ca^{2+}) at pH 5.1 (H_2O) or pH* 5.5 (^2H_2O) at 45 °C were analyzed as appropriate to the labeling pattern by multinuclear two-dimensional (2D) NMR experiments at spectrometer fields of 14.09 and 11.74 T: ^1H–^{13}C single-bond correlation ($^1H\{^{13}C\}$SBC); ^1H–^{13}C single-bond correlation with NOE relay ($^1H\{^{13}C\}$SBC-NOE); ^1H–^{13}C single-bond correlation with Hartmann–Hahn relay ($^1H\{^{13}C\}$SBC-HH); ^1H–^{13}C multiple-bond correlation ($^1H\{^{13}C\}$MBC); ^1H–^{15}N single-bond correlation ($^1H\{^{15}N\}$SBC); ^1H–^{15}N single-bond correlation with NOE relay ($^1H\{^{15}N\}$SBC-NOE). The results have assisted in spin system assignments and in identification of secondary structural elements. Nuclear Overhauser enhancements (NOE's) characteristic of antiparallel β-sheet ($d_{\alpha\alpha}$ NOE's) were observed in the $^1H\{^{13}C\}$-SBC-NOE spectrum of the nuclease ternary complex labeled uniformly with ^{13}C. NOE's characteristic of α-helix (d_{NN} NOE's) were observed in the $^1H\{^{15}N\}$SBC-NOE spectrum of the complex prepared from protein labeled uniformly with ^{15}N. The assignments obtained from these multinuclear NMR studies have confirmed and extended assignments based on $^1H\{^1H\}$ 2D NMR experiments [Wang, J., LeMaster, D. M., & Markley, J. L. (1990) *Biochemistry* (preceding paper in this issue)].

Staphylococcal nuclease has been studied for many years as a model system for investigations of structure–function relationships (Taniuchi & Anfinsen, 1967; Tucker et al., 1978, 1979; Evans et al., 1987; Hibler et al., 1987; Grissom & Markley, 1989). Detailed NMR[1] solution studies of the effects of inhibitor binding, conformational mobility, and mechanisms of protein folding require extensive spectral assignments. An early attempt to assign specific resonances in the 1D NMR spectrum of nuclease utilized selectively deuterated staphylococcal nuclease (Markley et al., 1978; Jardetzky et al., 1972) and selectively nitrated nuclease (Cohen et al., 1971). Histidine $^1H^{\epsilon 1}$ resonances have been assigned in 1D ^1H NMR spectra by using site-directed mutagenesis (Alexandrescu et al., 1988).

The application of 2D ^1H NMR techniques to small proteins has advanced rapidly (Wüthrich, 1986). The larger size of staphylococcal nuclease (17 kDa) has precluded the application of these techniques for the assignments of its ^1H spin systems. The approach we have found to be successful has relied heavily on random fractional deuteration (LeMaster & Richards, 1988) as described in the preceding paper (Wang et al., 1990) along with ^{13}C and ^{15}N labeling methods described here. $^1H\{^1H\}$ 2D NMR methods in conjunction with random fractional deuteration provided much of the information needed to elucidate proton spin systems and a large portion of the NOE information needed for sequential assignments and the elucidation of secondary structure. Uniform or specific labeling (with ^{13}C or ^{15}N) in conjunction with heteronuclear 2D NMR spectroscopy yielded information necessary for assigning the spin systems of long-chain amino acids. Heteronuclear 2D experiments with NOE relay provided additional key information about sequential assignments and secondary structure.

A somewhat different multinuclear NMR approach involving isotope labeling has been used by (Torchia et al., 1989) to achieve sequence-specific assignments and an analysis of

†Supported by Grant GM35976 from the National Institutes of Health. This study made use of the National Magnetic Resonance Facility at Madison which is supported in part by NIH Grant RR02301 from the Biomedical Research Technology Program, Division of Research Resources. Equipment in the facility was purchased with funds from the University of Wisconsin, the NSF Biological Biomedical Research Technology Program (DMB-8415048), the NIH Biomedical Research Technology Program (RR02301), the NIH Shared Instrumentation Program (RR02781), and the U.S. Department of Agriculture. Presented at the 30th Experimental Nuclear Magnetic Resonance Conference, Asilomar, CA, Apr 2–6, 1989.

‡Trainee supported by a Training Grant in Cellular and Molecular Biology (NIH GM07215).

[1] Abbreviations: COSY, 2D correlated spectroscopy; 2D, two dimensional; DQF, double quantum filtered; FID, free induction decay; IPTG, isopropyl β-D-thiogalactopyranoside; MOPS, 3-(*N*-morpholino)-propanesulfonic acid; NMR, nuclear magnetic resonance; NOE, nuclear Overhauser enhancement; NOESY, 2D NOE spectroscopy; nuclease H124L, mutant of the nuclease from *Staphylococcus aureus* (Foggi strain) (EC 3.14.7) in which the histidine at residue 124 has been replaced with leucine; H124L-TC, nuclease H124L–pdTp–Ca^{2+} ternary complex; [26% ul ^{13}C]H124L-TC, ternary complex made with nuclease enriched uniformly with ^{13}C to 26% isotope; [95% ul ^{15}N]H124L-TC, ternary complex made with nuclease enriched uniformly with ^{15}N to >95% isotope; [26% ul ^{13}C]Lys-H124L-TC, ternary complex made with nuclease that contains lysine enriched uniformly with ^{13}C to 26% isotope; pdTp, thymidine 3′,5′-bisphosphate; pH*, direct pH meter reading taken of a sample dissolved in ^2H_2O with an electrode calibrated with ordinary buffers in H_2O; TSP, 3-(trimethylsilyl)propionate-d_4; SDS–PAGE, sodium dodecyl sulfate–polyacrylamide gel electrophoresis. Cross-peak positions in spectra are given as x,y ppm where x is the horizontal axis and y is the vertical axis.

0006-2960/90/0429-102$02.50/0

the secondary structure of the pdTp–Ca^{2+} ternary complex with a different staphylococcal nuclease sequence.

Experimental Procedures

Protein Samples. Nuclease analogues uniformly labeled with ^{15}N or ^{13}C were overproduced in *Escherichia coli* strain BL21-(DE3) by means of the phage T7 promoter system (Studier & Moffatt, 1986). Nuclease H124L (identical with the nuclease isolated from the V8 strain of *Staphylococcus aureus*) was encoded by the plasmid pTSN2cc, originally provided by Dr. David LeMaster (Northwestern University) and subsequently modified in our laboratory to restore the plasmid copy control region. Uniform ^{15}N labeling was achieved by growing cultures in M9 medium (Maniatis et al., 1982) in which 99.8% ^{15}N enriched $(NH_4)_2SO_4$ (Isotec, Inc.) replaced NH_4Cl as the sole nitrogen source. Uniform ^{13}C enrichment was achieved by using noninducing MOPS media with 26% ul ^{13}C labeled algal protein hydrochloride hydrolysate (isolated from *Anabaena* 7120) supplied at 8 g/L in place of glucose as the sole carbon source. Nuclease production was initiated by the addition of IPTG. A crude extract was prepared by repeated freeze–thawing of the isolated cell pellets. Upon cell lysis, 1 M $CaCl_2$ was added to a final concentration of 50 mM. After this mixture was incubated at 37 °C for 15 min, the cell debris was removed by centrifugation, and the supernatant was purified as described previously (Alexandrescu et al., 1988). Typical yields were 40 mg of purified protein/L of culture. Samples were judged to be in excess of 95% pure by SDS–PAGE.

Specific labeling with lysine, methionine, or arginine was achieved by using a strain of *E. coli* auxotrophic for that amino acid. Specific labeling with [^{15}N]leucine was achieved by using a strain deficient in transaminase activity. In each case, H124L was overexpressed and purified according to the procedures described previously (Alexandrescu et al., 1988). [26% ul ^{13}C]lysine, [26% ul ^{13}C]arginine, and [26% ul ^{13}C]Met were isolated from the *Anabaena* 7120 protein hydrolysates by modification of the procedure of LeMaster and Richards (1982). [99% ^{15}N]-L-Leucine was purchased from Cambridge Isotope Laboratories.

Preparation of the nuclease ternary complex (H124L-TC) was as described in the accompanying paper (Wang et al., 1990). The pH of samples dissolved in H_2O was 5.1; the pH* of samples dissolved in ^2H_2O was 5.5. The labile protons of all ^{13}C-labeled nuclease samples were exchanged fully for deuterons by heating the samples in ^2H_2O solution for 45 min at 37 °C. Samples used for $^1H\{^{13}C\}$ NMR spectroscopy were dissolved in 100% ^2H_2O; samples used for $^1H\{^{15}N\}$ spectroscopy were dissolved in 90% H_2O/10% ^2H_2O.

NMR Spectroscopy. Two-dimensional $^1H\{^{13}C\}$ and $^1H\{^{15}N\}$ NMR data were collected on Bruker AM 500 or AM 600 spectrometers at a probe temperature of 45 °C. ^1H chemical shifts were measured relative to the water peak and are reported relative to TSP; ^{13}C chemical shifts were measured relative to 10% dioxane in ^2H_2O (taken as 67.8 ppm relative to TMS); ^{15}N chemical shifts were calibrated relative to 95% $(^{15}NH_4)_2SO_4$ in H_2O (taken as 21.6 ppm relative to the chemical shift of liquid ammonia).

(1) ^1H-Detected Heteronuclear Single-Bond ^1H–^{13}C and ^1H–^{15}N Chemical Shift Correlation Spectroscopy (^1H-$\{^{13}C,^{15}N\}$SBC). The following pulse sequence was used (Sklenar et al., 1987):

$$\begin{array}{ll} ^1H: & 90°\text{–}\tau\text{–}\quad -t_1/2\text{–}180°\text{–}t_1/2\text{–}\quad -\tau\text{–Acq}(t_2) \\ X: & \quad 90° \qquad\qquad\quad 90° \quad \text{decouple} \end{array}$$

The delay time τ was set to be $(1/2)^1J_{XH}$, i.e., 3.57 ms for the aliphatic region and 2.78 ms for the aromatic region of $^1H\{^{13}C\}$ spectra and 5.56 ms for $^1H\{^{15}N\}$ spectra. Separate data sets were collected for the aromatic and aliphatic regions of $^1H\{^{13}C\}$ spectra, and $^1H\{^{15}N\}$ data were acquired for only the amide region. The ^{13}C carrier frequency was adjusted to be at the center of the region of interest (aliphatic or aromatic). The ^{15}N carrier frequency was centered in the amide region. Water suppression in $^1H\{^{15}N\}$ experiments with samples in H_2O was achieved by presaturation during the ^1H relaxation delay. For each value of t_1, 4096 data points were collected in t_2. Prior to Fourier transformation, double zero-filling in the t_1 dimension was applied. Other spectral parameters are provided in the figure legends.

(2) ^1H-Detected Heteronuclear Single-Bond ^1H–^{13}C and ^1H–^{15}N Correlation with NOE Relay Spectroscopy (^1H-$\{^{13}C\}$SBC-NOE or $^1H\{^{15}N\}$SBC-NOE). $^1H\{^{13}C\}$SBC-NOE or $^1H\{^{15}N\}$SBC-NOE spectra were recorded with the pulse sequence (Shon et al., 1989)

$$\begin{array}{ll} ^1H: & 90°\text{–}\tau\text{–}\quad -t_1/2\text{–}180°\text{–}t_1/2\text{–}\quad -\tau\text{–}90°\text{–}\tau_m\text{–}90°\text{–Acq}(t_2) \\ X: & \quad 90° \qquad\qquad\quad 90° \quad \text{decouple} \end{array}$$

This pulse sequence is a combination of a ^1H-detected heteronuclear correlation scheme with a ^1H homonuclear NOE experiment. The experiments were performed with NOESY mixing times of τ_m = 200 and 250 ms, for both ^{13}C-labeled and ^{15}N-labeled nuclease H124L. Water suppression was applied during the ^1H relaxation delay time and the mixing time τ_m in ^1H–^{15}N heteronuclear experiments. The experimental setting and spectral parameters were identical with those of heteronuclear single-bond correlation experiments.

(3) ^1H-Detected Heteronuclear Multiple-Bond ^1H–^{13}C Correlation Spectroscopy ($^1H\{^{13}C\}$MBC). The experiment was performed with the pulse sequence (Bax et al., 1986)

$$\begin{array}{ll} ^1H: & 90°\text{–}\tau_1\text{–}\quad -\tau_2\text{–}\quad -t_1/2\text{–}180°\text{–}t_1/2\text{–}\quad -\text{Acq}(t_2) \\ ^{13}C: & \quad 90°\text{–}\tau_2\text{–}90° \qquad\qquad 90° \quad \text{decouple} \end{array}$$

The delay time τ_1 serves to eliminate single-bond correlations (τ_1 = 3.57 ms), while τ_2 is set to optimize two- and three-bond coupling (τ_2 = 70 ms). The data set consisted of 512 t_1 increments of 4096 data points each. Before Fourier transformation, double zero-filling was applied in the t_1 dimension. Following Fourier transformation, spectra were phased in the t_1 dimension and magnitude-calculated in the t_2 dimension.

(4) ^1H-Detected Heteronuclear Single-Bond ^1H–^{13}C Correlation with Hartmann–Hahn Relay Spectroscopy (^1H-$\{^{13}C\}$SBC-HH). The $^1H\{^{13}C\}$SBC-HH experiment used the pulse sequence (Oh et al., 1989)

$$\begin{array}{ll} ^1H: & 90°\ \text{–}\tau\text{–}\quad -t_1/2\text{–}180°\text{–}t_1/2\text{–}\quad -\tau\text{–SL}_x\text{–MLEV-17–SL}_x\text{–Acq}(t_2) \\ ^{13}C: & \quad 90° \qquad\qquad 90° \quad \text{decouple} \end{array}$$

The experiment was carried out separately for the aliphatic and aromatic regions. Data were collected with spin-lock mixing times of 40 and 70 ms. Other parameters for acquiring and processing data were as given above for the $^1H\{X\}$SBC experiment.

Results and Discussion

The application of 2D $^1H\{^{13}C\}$ and $^1H\{^{15}N\}$ NMR techniques in the study of H124L-TC provided a direct means for determining its secondary structure and facilitated spin system assignments. The $^1H\{^{13}C\}$SBC method suppresses signals from protons that are not directly bonded to ^{13}C and thus simplifies the 2D spectrum. Moreover, by combining the homonuclear Hartmann–Hahn data with the ^1H–^{13}C heteronuclear single-bond correlation data ($^1H\{^{13}C\}$SBC-HH), one obtains a hybrid spectrum that displays direct and relayed connectivities. This permits the ^{13}C chemical shifts that are characteristic

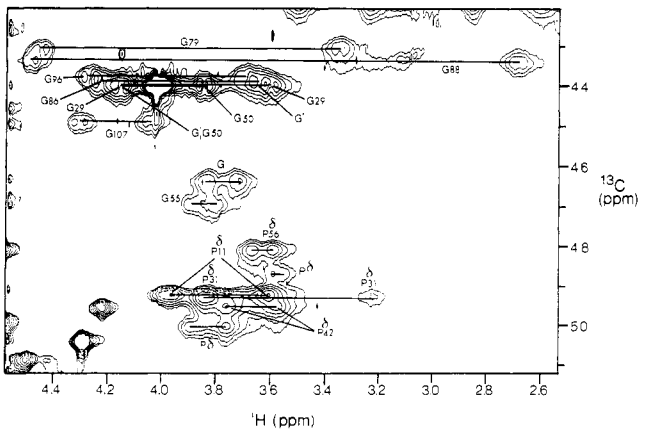

FIGURE 1: Portion of two-dimensional $^1H\{^{13}C\}$SBC spectrum of ^{13}C uniformly labeled staphylococcal nuclease ternary complex ([26% ul ^{13}C]H124L-TC) in ^2H_2O, recorded on a Bruker AM-600 spectrometer. A total of 96 FID's were collected for each t_1 value, and 512 blocks were recorded with an acquisition time of 0.32 s. The relaxation delay time was 1.8 s. Shifted sine bell filtering was used in t_1, and a Gaussian function was used in t_2. Single-bond correlation cross peaks assigned to glycine ($^1H^{\alpha}$–$^{13}C^{\alpha}$) and proline ($^1H^{\delta}$–$^{13}C^{\delta}$) are labeled by the one-letter amino acid code and residue number.

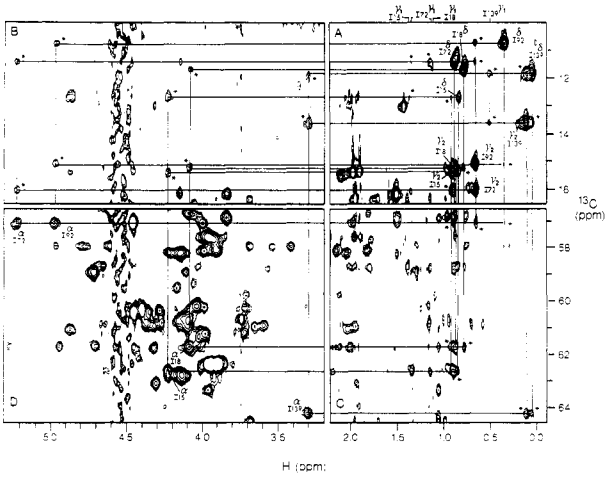

FIGURE 2: Four parts of the 500-MHz two-dimensional $^1H\{^{13}C\}$-SBC-NOE spectrum of ^{13}C-labeled staphylococcal nuclease ternary complex ([26% ul ^{13}C]H124L-TC) in ^2H_2O. 460 increments were recorded with 160 scans per t_1 value. The mixing time used for the NOE buildup was 0.25 s. The spin system assignments of isoleucines are presented. (A) Region containing $^1H^{\gamma_2}$–$^{13}C^{\gamma_2}$ and $^1H^{\delta}$–$^{13}C^{\delta}$ direct cross peaks and $^1H^{\gamma_1}$–$^{13}C^{\gamma_2,\delta}$ NOE relay cros peaks of isoleucine. (B) Region containing isoleucine $^1H^{\alpha}$–$^{13}C^{\gamma_2}$ and $^1H^{\alpha}$–$^{13}C^{\delta}$ NOE relay cross peaks. (C) Region containing isoleucine $^1H^{\gamma_2}$–$^{13}C^{\alpha}$ and $^1H^{\delta}$–$^{13}C^{\alpha}$ NOE relay cross peaks. (D) Region containing isoleucine $^1H^{\alpha}$–$^{13}C^{\alpha}$ direct cross peaks. The NOE relay cross peaks are indicated by asterisks.

of different amino acids to be used in making spin system assignments. In the $^1H\{^{15}N\}$SBC-NOE spectrum, one expects to observe NOE's betwen pairs of amide protons and between amide and side-chain protons. As a consequence, the experiment provides an excellent means of detecting the presence of α-helices, reverse turns, and β-sheets. Side-chain assignments can be obtained on the basis of the NOE relay between amide protons and side-chain protons. the $^1H\{^{13}C\}$SBC-NOE spectrum displays NOE connectivities between adjacent $^1H^{\alpha}$ protons, which allows one to identify antiparallel β-sheet structure. Connectivities between $^1H^{\alpha}$ and side-chain protons serve to extend the identification of spin systems. The combined use of specific ^{13}C labeling with $^1H\{^{13}C\}$SBC-NOE spectroscopy or specific ^{15}N labeling with $^1H\{^{15}N\}$SBC-NOE spectroscopy efficiently overcomes problems of overlap and degeneracy of cross peaks in the COSY and NOESY fingerprint regions.

Spin System Assignment by ^1H–^{13}C Experiments. It is well-known that ^{13}C chemical shifts are generally more diagnostic of individual amino acid residue types than ^1H chemical shifts. ^1H–^{13}C chemical shift correlations from heteronuclear 2D spectra thus facilitate spin system assignments. Through the combined use of a variety of proton-detected heteronuclear 2D experiments, numerous spin systems of H124L-TC have been identified and assigned to particular residues in the protein sequence. These assignments have confirmed and supplemented spin system assignments based on $^1H\{^1H\}$ 2D experiments (Wang et al., 1990). The ^{13}C and ^{15}N chemical shifts of H124L-TC are summarized in Table I. ^1H chemical shifts are given in the preceding paper (Wang et al., 1990). By utilizing these newly developed ^1H-detected heteronuclear experiments with labeled H124L-TC, additional spin system assignments were obtained and assignments made by $^1H\{^1H\}$ 2D experiments were confirmed and extended.

Ten glycine cross peaks were assigned completely from $^1H\{^{13}C\}$SBC data. The ^{13}C chemical shifts of these ten glycine residues are located within a small region which is well separated from the cluster of other ($^1H^{\alpha}$–$^{13}C^{\alpha}$) cross peaks (Figure 1) and are readily recognized by their two $^1H^{\alpha}$–$^{13}C^{\alpha}$ SBC cross peaks at a common ^{13}C chemical shift. Two of the glycines (Gly^{79} and Gly^{88} have unusually disparate $^1H^{\alpha_1}$ and $^1H^{\alpha_2}$ chemical shifts.

Two of the five isoleucine residues of H124L-TC could not be identified from $^1H\{^1H\}$ 2D experiments. However, the spin system of all five isoleucine residues can be identified in the $^1H\{^{13}C\}$SBC-NOE spectrum (Figure 2). The $^{13}C^{\delta}$ and $^{13}C^{\gamma_2}$ chemical shifts of isoleucine residues are expected to be present at high field in ω_1; therefore, it is very easy to recognize isoleucine ($^1H^{\delta}$–$^{13}C^{\delta}$) and ($^1H^{\gamma_2}$–$^{13}C^{\gamma_2}$) single-bond correlation cross peaks in this region (Figure 2A). An intraresidue NOE relay (Figure 2B,C) leads to ($^1H^{\alpha}$–$^{13}C^{\alpha}$) cross peaks in Figure 2D as indicated by solid lines. As a consequence, the (^1H–^{13}C) single-bond correlation cross peaks of all five isoleucine residues were distinguished. A few Hartmann–Hahn relay peaks shown in the $^1H\{^{13}C\}$SBC-HH spectrum (Figure 3A) lend further support to these assignments.

Threonine ($^1H^{\beta}$–$^{13}C^{\beta}$) single-bond correlation cross peaks are expected in a characteristic region which makes it easy to identify their spin systems from $^1H\{^{13}C\}$SBC-NOE data. Associated with the ^{13}C chemical shift of each threonine ($^1H^{\beta}$–$^{13}C^{\beta}$) single-bond correlation cross peak are two NOE cross peaks at $^1H^{\alpha}$–$^{13}C^{\beta}$ and $^1H^{\gamma}$–$^{13}C^{\beta}$ (Figure 4A,B). The spin system of one threonine (Thr^{41}), which was not observed in $^1H\{^1H\}$ 2D spectra, was identified unambiguously by combining $^1H\{^{13}C\}$SBC-HH and $^1H\{^{13}C\}$SBC-NOE data. The $^1H\{^{13}C\}$SBC-HH spectrum clearly showed evidence for ^1H–^{13}C scalar coupling between a $^1H^{\alpha}/^{13}C^{\alpha}$ cross peak at 5.17,57.0 ppm and a $^1H^{\beta}$–$^{13}C^{\beta}$ cross peak at 4.25,66.6 ppm (Figure 3B). The $^1H\{^{13}C\}$SBC-NOE spectrum (Figure 4A) showed one NOE relay cross peak at 5.14,66.5 ppm which connected these two direct cross peaks. Data in Figure 4B allowed these chemical shifts to be linked to the $^1H^{\gamma}$ (1.18 ppm) of Thr^{41}. Thr^{62} has uncommon chemical shift values ($^1H^{\alpha}$ = 3.6 ppm; $^1H^{\beta}$ = 4.12 ppm) as confirmed by observing the connectivity network: i.e., the rectangle formed by direct cross peaks $^1H^{\alpha}$–$^{13}C^{\alpha}$ and $^1H^{\beta}$–$^{13}C^{\beta}$ at 3.6,66.1 and 4.12,66.5 ppm and NOE relay cross peaks $^1H^{\beta}$–$^{13}C^{\alpha}$ and $^1H^{\alpha}$–$^{13}C^{\beta}$ at 4.12,66.1 and 3.6,66.5 ppm (Figure 4A).

Two- and three-bond correlation cross peaks from alanine residues ($^1H^{\beta}$–$^{13}C^{\alpha}$ and $^1H^{\beta}$–$^{13}C'$) are located in the upfield region of the proton dimension of the $^1H\{^{13}C\}$MBC spectrum

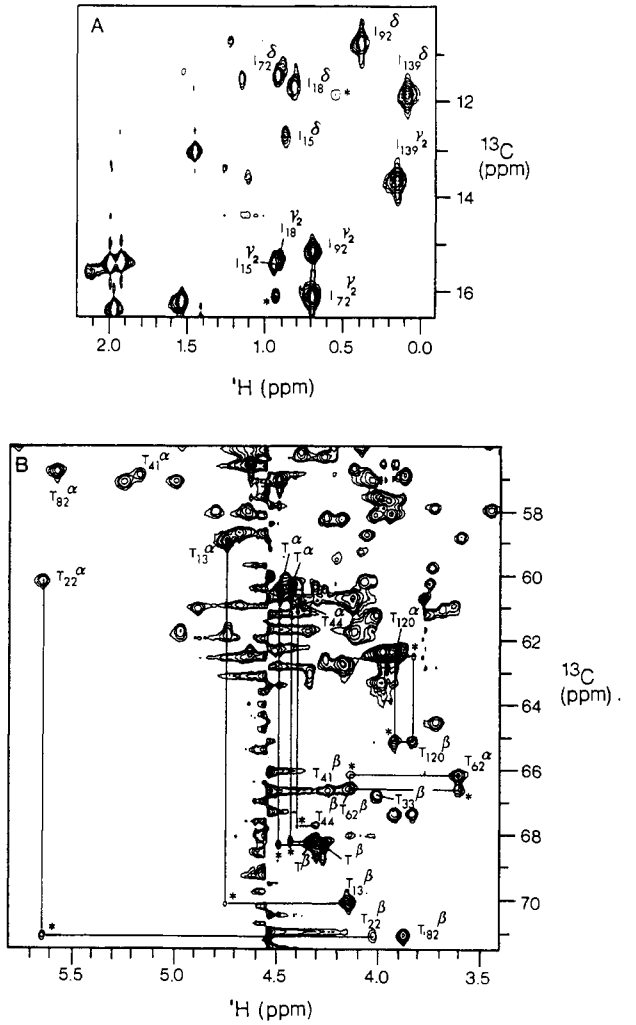

FIGURE 3: Two parts of the 600-MHz two-dimensional $^{1}H\{^{13}C\}$-SBC-HH spectrum of ^{13}C-labeled staphylococcal nuclease ternary complex ([26% ul ^{13}C]H124L-TC). The spectral range covered only the aliphatic region. Data were collected in 512 blocks, and 128 scans were taken for each t_1 value. (A) Region of isoleucine $^{1}H^{\gamma 2}$–$^{13}C^{\gamma 2}$ and $^{1}H^{\delta}$–$^{13}C^{\delta}$ direct cross peaks. Relayed cross peaks are indicated by asterisks. (B) Region containing threonine $^{1}H^{\alpha}$–$^{13}C^{\alpha}$ and $^{1}H^{\beta}$–$^{13}C^{\beta}$ direct cross peaks. Relayed $^{1}H^{\beta}$–$^{13}C^{\alpha}$ and $^{1}H^{\alpha}$–$^{13}C^{\beta}$ cross peaks of threonine are indicated by asterisks.

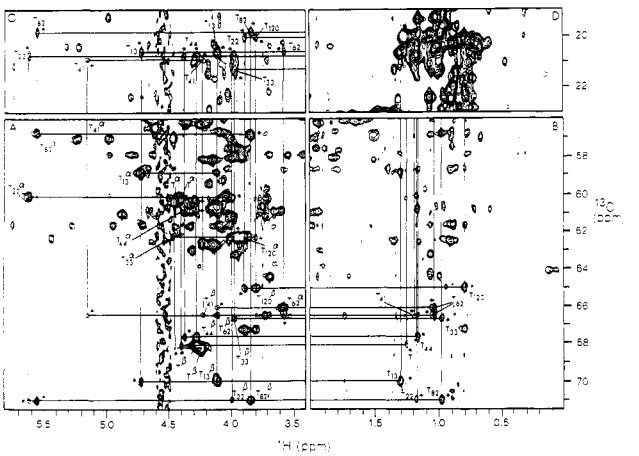

FIGURE 4: Four parts of the aliphatic region of the $^{1}H\{^{13}C\}$SBC-NOE spectrum of the ^{13}C-labeled staphylococcal nuclease ternary complex ([26% ul ^{13}C]H124L-TC) illustrating threonine spin system assignments. (A) Region of $^{1}H^{\alpha}$–$^{13}C^{\alpha}$ and $^{1}H^{\beta}$–$^{13}C^{\beta}$ direct cross peaks and $^{1}H^{\alpha}$–$^{13}C^{\beta}$ and $^{1}H^{\beta}$–$^{13}C^{\alpha}$ NOE relay cross peaks (indicated by asterisks). (B) Region of threonine $^{1}H^{\gamma}$–$^{13}C^{\beta}$ and $^{1}H^{\gamma}$–$^{13}C^{\alpha}$ relay NOE cross peaks. (C) Region of threonine $^{1}H^{\alpha}$–$^{13}C^{\gamma}$ and $^{1}H^{\beta}$–$^{13}C^{\gamma}$ NOE relay cross peaks. (D) Region of threonine $^{1}H^{\gamma}$–$^{13}C^{\gamma}$ direct cross peaks.

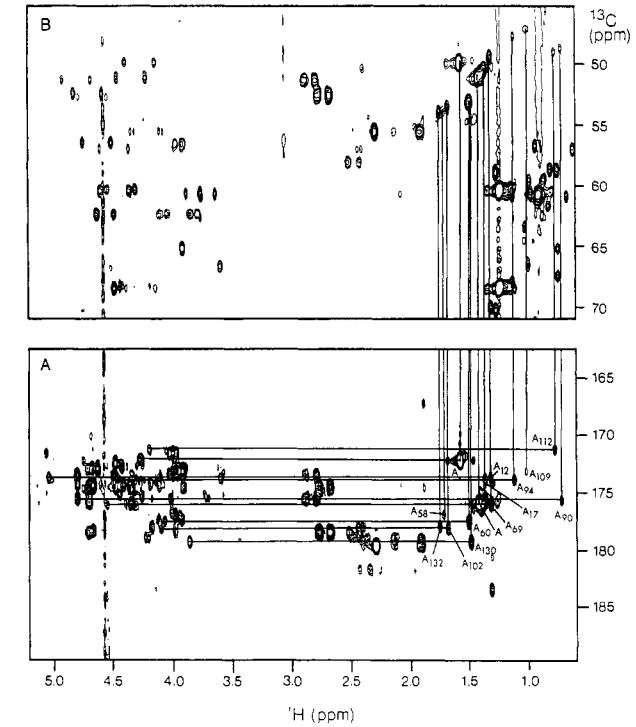

FIGURE 5: Two regions of the $^{1}H\{^{13}C\}$MBC spectrum of the ^{13}C-labeled staphylococcal nuclease ternary complex ([26% ul ^{13}C]H124L-TC) recorded on a Bruker AM-600 spectrometer with 482 increments and 112 scans for each t_1 value. The spectrum is presented in the mixed mode, with pure absorption in ω_1 and absolute value in ω_2. The delay time was set to 70 ms. A Gaussian window function was used in t_2 and t_1. (A) Region of alanine $^{1}H^{\alpha}$–$^{13}C'$ and $^{1}H^{\beta}$–$^{13}C'$ two- and three-bond correlation cross peaks. (B) Region of alanine $^{1}H^{\beta}$–$^{13}C^{\alpha}$ two-bond correlation cross peaks.

(Figure 5). The methyl proton to carbonyl carbon correlation distinguishes cross peaks corresponding to alanine spin systems from those of other methyl-containing amino acids (Ile, Leu, Met, Thr, Val). Moreover, alignment of the $^{1}H^{\beta}$–$^{13}C'$ and $^{1}H^{\beta}$–$^{13}C^{\alpha}$ cross peaks along the $^{1}H^{\beta}$ chemical shift in the $^{1}H\{^{13}C\}$MBC spectrum is highly diagnostic for alanine. The 14 alanine ($^{1}H^{\beta}$–$^{13}C'$) cross peaks were assigned readily. Extension along the $^{13}C'$ chemical shift identifies the alanine $^{1}H^{\alpha}$. Alanine spin systems determined by this approach were fully consistent with ^{1}H homonuclear HOHAHA data.

In the $^{1}H\{^{13}C\}$SBC spectrum, the pairs of $^{1}H^{\delta_1}$–$^{13}C^{\delta}$ and $^{1}H^{\delta_2}$–$^{13}C^{\delta}$ single-bond correlation cross peaks from six proline residues are concentrated in the 3.1–4.0,47–50 ppm region (Figure 1). An NOE connectivity between a proline $^{1}H^{\delta}$ and the $^{1}H^{\alpha}$ of the preceding residue is diagnostic for the trans X–Pro peptide bond conformation (Wüthrich, 1986). Several such NOE cross peaks were observed for H124L-TC. The $^{1}H^{\alpha}$–$^{13}C^{\alpha}$ single-bond correlation cross peaks of Gln^{30} and Glu^{10} (assigned from the $^{1}H^{\alpha}$ chemical shifts) (Wang et al., 1990) and Thr^{41} build up NOE's with $^{1}H^{\delta}$ signals assigned to Pro^{31}, Pro^{11}, and Pro^{42}, respectively (Figure 6B). One pair of $^{1}H^{\delta_1}$–$^{13}C^{\delta}$ and $^{1}H^{\delta_2}$–$^{13}C^{\delta}$ cross peaks at 3.58,47.9 and 3.66,47.9 ppm show an NOE connectivity to the $^{1}H^{\alpha}$–$^{13}C^{\alpha}$ cross peak of one glycine at 3.78,47.9 ppm. These peaks are readily assigned to the unique dipeptide Gly^{55}-Pro^{56}.

Staphylococcal nuclease H124L contains 23 lysine and 5 arginine residues. The resulting heavy overlap in the $^{1}H^{\gamma}$–$^{1}H^{\delta}$ region precluded their identification from $^{1}H\{^{1}H\}$ 2D spectra. Spectral simplification afforded by specific ^{13}C labeling of lysine (Figure 7) or arginine (not shown) residues of H124L-TC allowed us to identify the $^{1}H^{\alpha}$–$^{13}C^{\alpha}$ cross peaks of these residues in the $^{1}H\{^{13}C\}$SBC spectrum (Figure 6A).

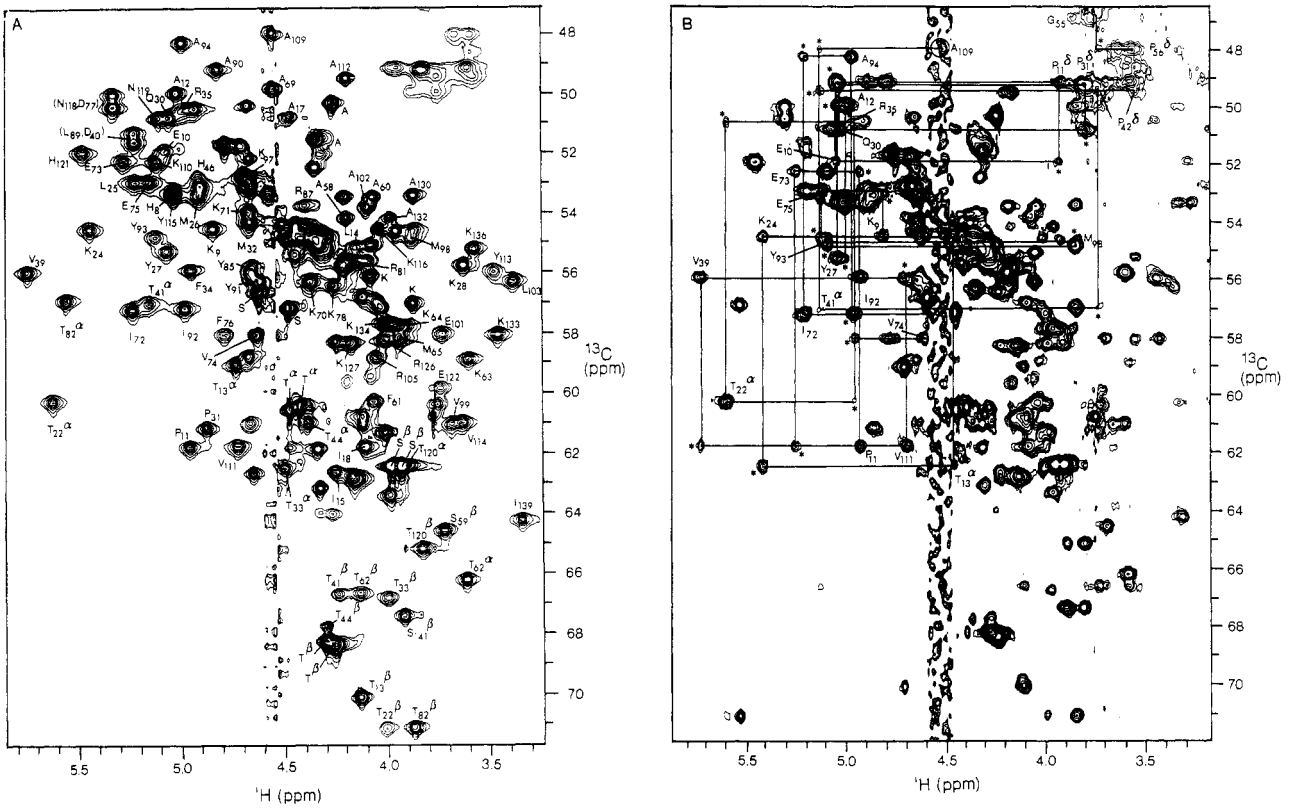

FIGURE 6: Comparison of $^{1}H\{^{13}C\}$SBC and $^{1}H\{^{13}C\}$SBC-NOE spectra of the ^{13}C-labeled staphylococcal nuclease ternary complex ([26% ul ^{13}C]H124L-TC). The NOE relay cross peaks provide interresidue connectivities that are diagnostic for secondary structural elements. (A) A portion of the aliphatic region of the 600-MHz $^{1}H\{^{13}C\}$SBC spectrum. All the cross peaks shown are from amino acid $^{1}H^{\alpha}$–$^{13}C^{\alpha}$ direct correlations, except for serine and threonine which yield $^{1}H^{\beta}$–$^{13}C^{\beta}$ direct correlations in this region. Assigned cross peaks are labeled by the one-letter amino acid code and residue number. (B) A portion of the aliphatic region of the 500-MHz $^{1}H\{^{13}C\}$SBC-NOE spectrum. This region shows amino acid $^{1}H^{\alpha}$–$^{13}C^{\alpha}$ direct cross peaks and interresidue $^{1}H^{\alpha}_{i}$–$^{13}C^{\alpha}_{j}$ NOE relay cross peaks. All identified interstrand $d_{\alpha\alpha}$ NOE connectivities are indicated except for that between Thr^{82} and Gly^{88}, which is outside the region plotted in the figure. All NOE relay cross peaks are indicated by asterisks. Additional labeled peaks correspond to proline $^{1}H^{\delta}$–$^{13}C^{\delta}$ direct cross peaks and $^{1}H^{\delta}_{i}$–$^{13}C^{\alpha}_{i-1}$ NOE relay cross peaks from trans X_{i-1}-Pro_i linkages.

These identifications facilitated sequence-specific assignments and secondary structural analysis.

All the aromatic amino acid residues of H124L-TC were assigned fully by combining ^{1}H homonuclear and $^{1}H\{^{13}C\}$ heteronuclear experiments. Assignments are indicated in Figure 6A. A discussion of the aromatic assignments will be presented separately (J. Wang, A. P. Hinck, S. N. Loh, and J. L. Markley, unpublished results).

Main-Chain Sequential Assignments by Means of ^{1}H–^{15}N Experiments. The $^{1}H^{\alpha}$–^{15}N and $^{1}H^{\beta}$–^{15}N regions of the $^{1}H\{^{15}N\}$SBC-NOE spectrum of [95% ul ^{15}N]H124L-TC reveal mainly ($^{1}H^{\alpha}_{i}$, $^{1}H^{\beta}_{i}$)–$^{1}H^{N}_{i}$ NOE connectivities to the $^{15}N_i$ chemical shift and ($^{1}H^{\alpha}_{i}$, $^{1}H^{\beta}_{i}$)–$^{1}H^{N}_{i+1}$ NOE connectivities to the $^{15}N_{i+1}$ chemical shift. Occasional relayed cross peaks indicate ($^{1}H^{\gamma}_{i}$, $^{1}H^{\delta}_{i}$)–$^{1}H^{N}_{i}$ NOE's. These cross peaks provide the same information as found in the ($^{1}H^{\alpha}$, $^{1}H^{\beta}$, $^{1}H^{\gamma}$)–$^{1}H^{N}$ connectivity regions of $^{1}H\{^{1}H\}$ COSY, RCT-COSY, and NOESY spectra obtained in H_2O. However, in the $^{1}H\{^{15}N\}$SBC-NOE spectrum all cross peaks have the ^{15}N chemical shift on one axis, whose dispersion serves to remove ambiguities commonly observed in $^{1}H\{^{1}H\}$ 2D spectra when cross peaks overlap, or are too close to the diagonal. Furthermore, since H124L-TC has a high content of α-helix, strong sequential NOE connectivities characteristic of α-helix [$d_{\beta N}(i,i)$ and $d_{\beta N}(i,i+1)$] (Englander et al., 1987) are expected. We have observed a large number of cross peaks in the $^{1}H^{\beta}$–^{15}N region. A sequential walk in this region starts from the NOE cross peak $^{1}H^{\beta}_{i}$–$^{15}N_i$ at the $^{15}N_i$ chemical shift. A vertical line leads to the NOE relay cross peak $^{1}H^{\beta}_{i}$–$^{15}N_{i+1}$ at the $15N_{i+1}$ chemical shift. A horizontal line goes from this NOE cross peak to the NOE relay cross peak $^{1}H^{\beta}_{i+1}$–$^{15}N_{i+1}$ at the $^{15}N_{i+1}$ chemical shift. Continuation of these steps give the $d_{\beta N}$ sequential walk.

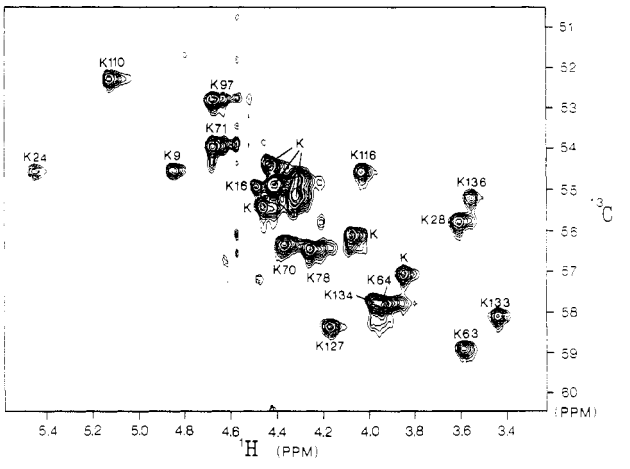

FIGURE 7: Portion of the 500-MHz $^{1}H\{^{13}C\}$SBC spectrum of the staphylococcal nuclease ternary complex labeled selectively with [^{13}C]lysine ([26% ul ^{13}C]Lys-H124L-TC). The spectrum was recorded with 512 blocks and 64 scans for each t_1 value. All 23 lysine $^{1}H^{\alpha}$–$^{13}C^{\alpha}$ direct cross peaks are resolved. Assigned cross peaks are labeled in the figure.

Analysis of $d_{\beta N}$ NOE cross peaks reveals one long $d_{\beta N}$ sequential walk as shown in Figure 8A. In accord with the previous classification of $^{1}H^{\alpha}$ chemical shifts to different amino acid types, this sequence was assigned to Val^{99}–Gln^{106}. One $^{1}H^{\beta}$–^{15}N NOE relay cross peak of Val^{99} at 1.8,136.8 ppm

Table I: ^{13}C and ^{15}N Resonance Assignments of Staphylococcal Nuclease H124L Ternary Complex at 45 °C[a]

	^{15}N	$^{13}C^{\alpha}$	$^{13}C^{\beta}$	$^{13}C^{\gamma}$	$^{13}C^{\delta}$		^{15}N	$^{13}C^{\alpha}$	$^{13}C^{\beta}$	$^{13}C^{\gamma}$	$^{13}C^{\delta}$
Leu 7	121.9*					Asp 77	124.1*	49.9/50.4*			
His 8		53.4*	29.5			Lys 78	120.0	56.4			
Lys 9	124.7*	54.5				Gly79	111.6	43.1			
Glu 10	123.5*	51.8				Gln 80					
Pro 11		61.7*			49.2	Arg 81	121.3	55.6			
Ala 12	120.7*	49.9	17.9			Thr 82	108.2	56.8	71.1	19.9	
Thr 13	109.8	58.9	70.0	20.7		Asp 83					
Leu 14	126.1*	55.1				Lys 84	125.6*				
Ile 15		62.5		γ_2 15.3	12.7	Tyr 85	120.9	55.9	36.7		
Lys 16	114.9*	54.9				Gly 86	109.7*	43.8			
Ala 17	130.0*	50.7	16.7			Arg 87	122.2	53.7			
Ile 18	124.8	61.7		γ_2 15.2	11.7	Gly 88	109.1*	43.4			
Asp 19	119.3					Leu 89	126.9*	51.2/51.5*			
Gly 20						Ala 90	120.9	49.1	20.2		
Asp 21	111.9					Tyr 91	123.0*	56.2	36.2*		
Thr 22	118.0	60.1	71.1	20.8		Ile 92		57.2		γ_2 15.1	10.7
Val23	121.1*					Tyr 93	127.2*	54.7	36.2		
Lys 24	128.1*	54.5				Ala 94	126.6	48.2	18.5		
Leu25	127.9*	52.9				Asp 95	128.2				
Met 26	122.9	53.4	30.7	30.2		Gly 96	103.7	43.7			
Tyr 27	130.4*	55.2	40.2			Lys 97	122.2	52.7			
Lys 28	128.3	55.7				Met 98	127.6*	54.8	32.9	27.3	
Gly 29	103.0	43.9				Val 99	136.8	61.1*		20.3; 21.2	
Gln 30	120.2	50.7				Asn 100	109.0				
Pro 31		61.1			49.3	Glu 101	113.6	58.0			
Met 32	126.3*	54.3*	35.6	30.5		Ala 102	123.7	53.7	16.7		
Thr 33		62.3	66.7	21.3		Leu 103	116.3	56.3			
Phe 34	126.7*	55.8	40.8			Val 104	117.2				
Arg 35	125.5*	50.5				Arg 105	123.6	58.8			
Leu 36	125.3*					Gln 106	112.8				
Leu 37	122.9*					Gly 107	107.5	44.9			
Leu 38	112.6*					Leu 108	115.9				
Val 39	104.6	55.9				Ala 109	114.2	47.9	20.0		
Asp 40		51.2/51.5*				Lys 110		52.2			
Thr 41		56.9	66.6	21.0		Val 111	124.5*	61.6			
Pro 42					49.5	Ala 112	132.1*	49.4	18.6		
Glu 43						Tyr 113	111.3*	55.9			
Thr 44		60.8	67.6	20.8		Val 114	120.2*	61.0*		17.7; 18.6	
Lys 45						Tyr 115	131.1*	53.3	36.8		
His 46		52.8*	29.0			Lys 116	126.1*	54.5			
Pro 47						Pro 117					
Lys 48						Asn 118	129.4	49.9/50.4*			
Lys 49						Asn 119	118.5	50.7*			
Gly 50		44.0				Thr 120	124.6	62.3	65.1	20.1	
Val 51						His 121		51.9*	27.2		
Glu 52						Glu 122	120.9	59.7*			
Lys 53						Gln 123	118.4				
Tyr 54		54.7	37.1			Leu 124	122.0				
Gly 55		46.9				Leu 125	119.6				
Pro 56					48.1	Arg 126	119.7	58.2			
Glu 57						Lys 127	122.9	58.4			
Ala 58	124.7	54.1	16.8			Ser 128	118.4				
Ser 59	112.7		64.4*			Glu 129	125.6				
Ala 60	119.7	53.4	16.7			Ala 130	120.5	53.4	16.1		
Phe 61	122.1	60.1	38.3			Gln 131	118.8				
Thr 62	120.8	66.1	66.5	20.7		Ala 132	123.8	54.1	17.1		
Lys 63	120.7	58.9				Lys 133	118.1	58.1			
Lys 64	118.1	57.8				Lys 134	122.9	57.7			
Met 65	117.0	58.1	31.5	31.1		Glu 135	117.1				
Val 66	108.5					Lys 136	117.5	55.1			
Glu 67	121.8					Leu 137	118.0				
Asn 68	114.3					Asn 138	119.6*				
Ala 69	122.1	49.8	17.8			Ile 139	125.4	64.1		γ_2 13.6	11.8
Lys 70	126.4	56.3				Trp 140	120.4	53.5	28.5		
Lys 71	121.9	53.9				Ser 141	116.7		67.3		
Ile 72	129.8	57.2		γ_2 16.0	11.4	Glu 142	122.0				
Glu 73		52.2				Asp 143	120.1				
Val 74	118.1*	58.0		18.8; 20.1							
Glu 75		52.9									
Phe 76		58.0	38.2								

[a] ^{13}C data were collected at pH* 5.5 in ^2H_2O solution; ^{15}N data were collected at pH 5.1 in H_2O solution. Asterisks indicate ^{13}C and ^{15}N resonances that could be assigned readily by $^1H\{^{13}C\}$ or $^1H\{^{15}N\}$SBC correlations on the basis of ^1H assignments. Methionine $^{13}C^{\epsilon}$ assignments are as follows: Met^{26}, 15.4 ppm; Met^{32}, 15.3 ppm; Met^{65}, 16.3 ppm; Met^{98}, 13.0 ppm.

connects vertically to a $^1H^{\beta}$–^{15}N NOE relay cross peak of Asn^{100} at 1.8,109.0 ppm; this, in turn, connects horizontally to a $^1H^{\beta}$–^{15}N NOE relay cross peak at 2.79,109.0 ppm. We conclude that the $^1H^{\beta}$ of Val^{99} is at 1.8 ppm and that the $^1H^{\beta}$

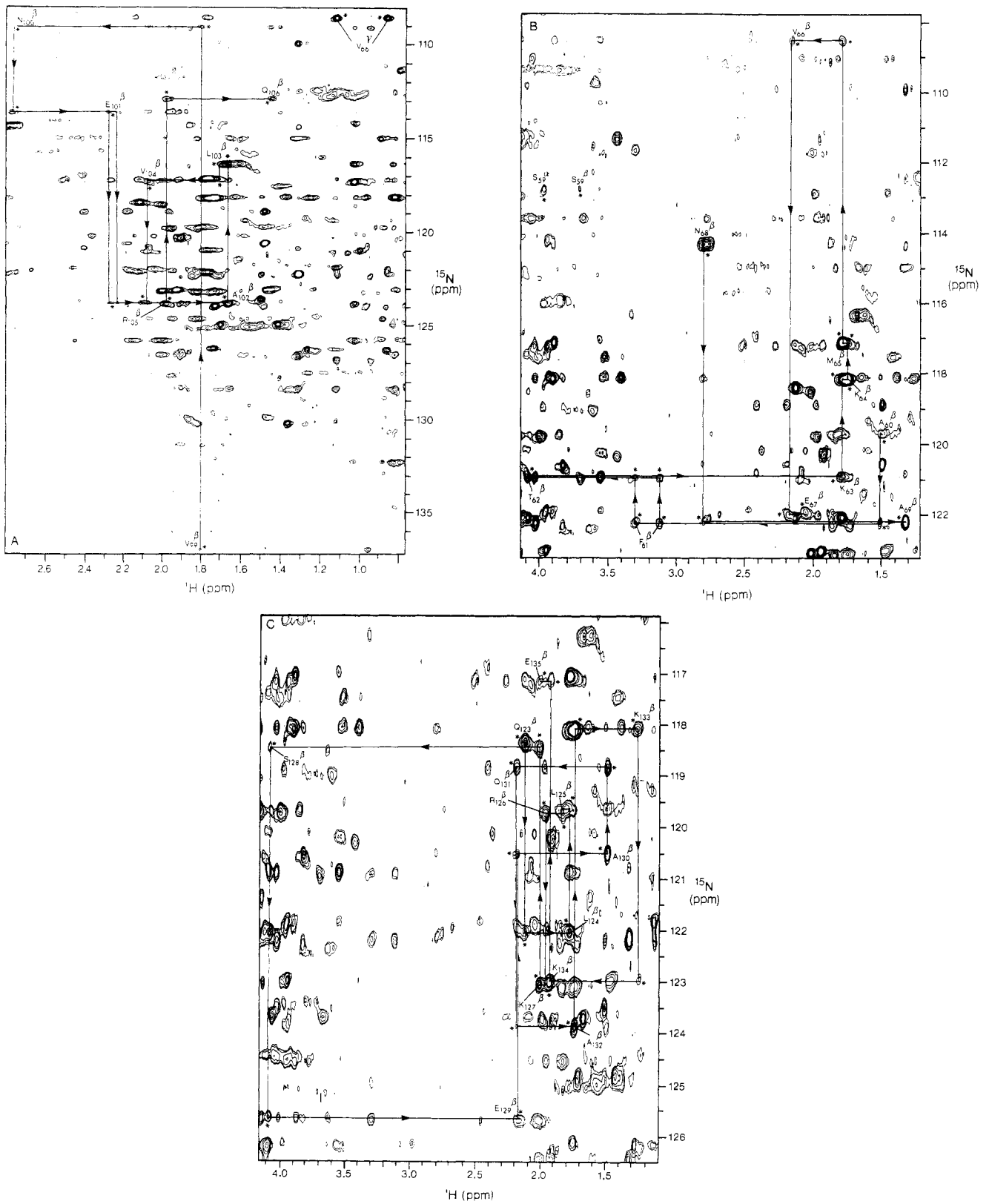

FIGURE 8: $^{1}H^{\beta}$–$^{1}H^{N}$ connectivity region of the $^{1}H\{^{15}N\}$SBC-NOE spectrum of ^{15}N-labeled staphylococcal nuclease ternary complex ([95% ul ^{15}N]H124L-TC). 346 increments were collected on a Bruker AM-600 spectrometer with 192 scans for each t_1 value. The NOE mixing time was set to 250 ms. Shifted sine bell filtering was used in t_1 and a Gaussian function in t_2. (A) ^{15}N-Assisted $d_{\beta N}$ sequential NOE connectivities assigned to Val^{99}–Gln^{106}. (B) ^{15}N-Assisted $d_{\beta N}$ sequential NOE connectivities assigned to Ala^{60}–Ala^{69}. (C) ^{15}N-Assisted $d_{\beta N}$ sequential NOE connectivities assigned to Gln^{123}–Glu^{135}.

of Asn^{100} is at 2.79 ppm. As shown in Figure 8A, this sequential walk yields the $^{1}H^{\beta}$ chemical shifts of residues involved in the segment Val^{99}–Gln^{106}. Sequential connectivities from Ala^{60} to Ala^{69} (Figure 8B) and from Gln^{123} to Glu^{135} (Figure 8C) were determined in the same fashion.

A number of $^{1}H^{\gamma}$–^{15}N NOE relay cross peaks were also observed clearly in the $^{1}H^{\gamma}$–^{15}N connectivity region. Val^{66} has an ^{15}N chemical shift of about 108.5 ppm. The NOE relay cross peak between $^{1}H^{N}$ and $^{1}H^{\gamma}$ of Val^{66} should lie on a horizontal line at the ^{15}N chemical shift of Val^{66} (108.5 ppm).

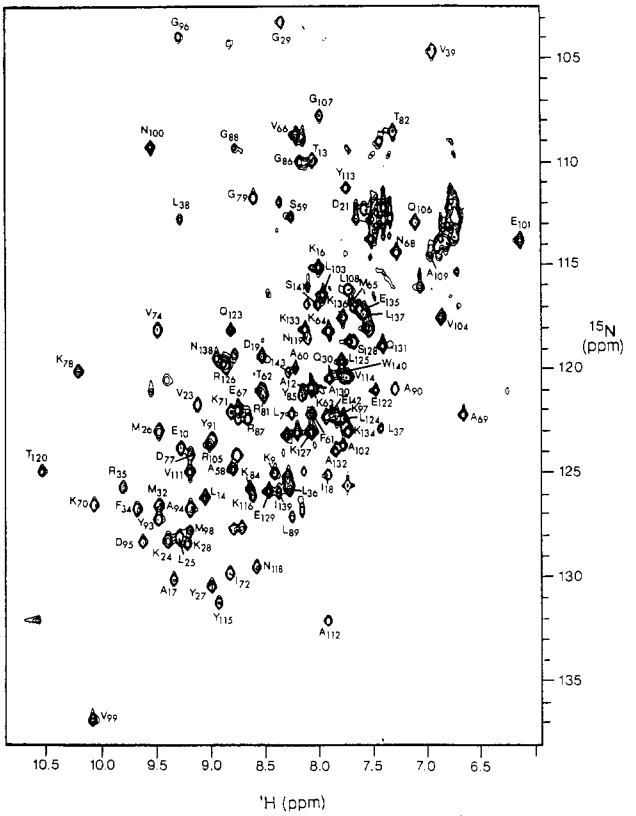

FIGURE 9: Complete $^{1}H^{N}$–^{15}N correlation region of the $^{1}H\{^{15}N\}$SBC spectrum of ^{15}N-labeled staphylococcal nuclease ternary complex ([95% ul ^{15}N]H124L-TC). The spectrum was recorded on a Bruker AM-500 spectrometer with 442 blocks and 136 scans for each t_1 value. The assigned cross peaks are labeled in the figure.

The strong cross peaks (Figure 8A) at 0.85,108.5 and 1.13,108.5 ppm were assigned on the basis of their chemical shifts to $^{1}H^{\gamma}$–^{15}N NOE relay connectivities of Val^{66}. The Val^{66} spin system was not identified by $^{1}H\{^{1}H\}$ 2D experiments.

Ser^{59} and Ser^{128} are involved in two different α-helical domains. Their $^{1}H^{\alpha}$ resonances were assigned by sequential NOE's, but each of them showed only one $^{1}H^{\alpha}$–$^{1}H^{\beta}$ cross peak in ^{1}H COSY spectra. Figure 8B,C shows that amino acid residues Ser^{59} and Ser^{128} each present only one $^{1}H^{\beta}$–^{15}N cross peak. This result shows that the two $^{1}H^{\beta}$'s of Ser^{59} likely have degenerate chemical shifts (at 3.74 ppm) as do the two $^{1}H^{\beta}$'s of Ser^{128} (at 4.1 ppm).

Spin system assigments of leucine proved difficult from $^{1}H\{^{1}H\}$ 2D spectra. However, by use of ^{15}N specific labeling, the 12 leucine residues of nuclease H124L have been identified in a $^{1}H\{^{15}N\}$SBC spectrum (not shown). The leucine cross peaks are indicated in Figure 9. The leucine $^{1}H^{N}$ chemical shifts derived from these data assisted with assignment of $^{1}H^{N}$–$^{1}H^{\alpha}$ cross peaks in the COSY fingerprint region. The $^{1}H^{N}$–^{15}N cross peaks assigned to leucine on the basis of selective labeling served as reference points for d_{NN} sequential assignments based on $^{1}H\{^{15}N\}$SBC-NOE data (see below).

Assignment of Three α-Helical Segments by $^{1}H\{^{15}N\}$SBC-NOE Spectroscopy. The amide region of the $^{1}H\{^{15}N\}$SBC-NOE spectrum shows $^{1}H^{N}$–^{15}N direct connectivity peaks plus additional cross peaks resulting from $^{1}H^{N}$–$^{1}H^{N}$ NOE's. The latter provide information equivalent to that of the amide region of a $^{1}H\{^{1}H\}$ NOESY (H_2O) spectrum. The NOE relay cross peaks arise most commonly from sequential connectivities between neighboring $^{1}H^{N}$ protons along the backbone, $d_{NN}(i,i+1)$, but can also arise from long-range nonsequential connectivities between $^{1}H^{N}$ protons of residues involved in secondary structural elements. Two equivalent NOE relay cross peaks usually are observed for every pair of direct $^{1}H^{N}$–^{15}N cross peaks. These four cross peaks form a rectangle with the direct and NOE relay cross peaks on opposite diagonals. Sequential connectivities give rise to a network of rectangles. Three sequentially related direct peaks define two rectangles which have as a common corner the direct $^{1}H^{N}$–^{15}N cross peak of the middle residue. Therefore, by linking all such common corner cross peaks, one obtains a sequential walk based on $d_{NN}(i,i+1)$ connectivities.

The following procedure is used to identify ^{15}N-assisted d_{NN} sequential connectivities in a $^{1}H\{^{15}N\}$SBC-NOE spectrum: (1) Relay peaks are identified that link a direct ($^{1}H^{N}$–^{15}N) cross peak a to a sequentially related direct ($^{1}H^{N}$–^{15}N) cross peak b. These four peaks lie on a rectangle whose sides are along ω_1 and ω_2. (2) One then searches from cross peak b along the sides of the rectangle and along their extensions for an additional relay peak that will link the rectangle from residues a and b to one from residues b and c. The additional relay peak may be on a side of the first rectangle or external to it. (3) The search is repeated from the newly identified direct cross peak so as to extend the sequence.

Three ^{15}N-assisted d_{NN} sequential walks were observed in the $^{1}H^{N}$–^{15}N connectivity region of the $^{1}H\{^{15}N\}$SBC-NOE spectrum of [95% ul ^{15}N]H124L-TC. The longest such sequential walk is indicated by solid lines in Figure 10A. The direction of the sequential walk is indicated by arrows. Identifications of residues along this path based on their $^{1}H^{N}$ chemical shifts assign this sequence to an α-helix running from Gln^{122} to Leu^{137}. The $^{1}H^{N}$ chemical shifts of Lys^{135} and Leu^{137} are very similar, and their d_{NN} cross peaks overlap in the $^{1}H\{^{1}H\}$ NOESY (H_2O) spectrum (Wang et al., 1990). However, the ^{15}N chemical shifts of these two residues are well separated so that the d_{NN} NOE connectivity is easily distinguished in the $^{1}H\{^{15}N\}$SBC-NOE spectrum. Other assignments in this helix confirm NOESY data (Wang et al., 1990).

A second sequential walk is presented in Figure 10B. Along the proton dimension, every step of this ^{15}N-assisted d_{NN} sequential walk is consistent with the NOESY ^{1}H d_{NN} connectivities previously obtained for the α-helix, Ala^{58}–Ala^{69}. The $^{1}H^{N}$ chemical shift values of Ser^{59} and Ala^{60} are very similar, such that, the d_{NN} NOE cross peaks between them are located close to the NOESY diagonal. As indicated in Figure 10B, the direct $^{1}H^{N}$–^{15}N cross peak of Ser^{59} is at 8.26,112.7 ppm and that of Ala^{60} is at 8.22,119.67 ppm. The 6.9 ppm difference between the ^{15}N chemical shifts of these adjacent residues makes the ^{15}N-assisted d_{NN} connectivity easy to recognize.

A third long ^{15}N-assisted d_{NN} sequential walk of ten residues is shown in Figure 10C. The steps of the sequential walk are the same as those assigned to the α-helix Val^{99}–Gly^{107} from NOESY data (Wang et al., 1990).

The ^{15}N assignments of the amino acid residues involved in these three α-helices are listed in Table I. The chemical shifts of amide protons identified in this study are presented in the preceding paper (Wang et al., 1990).

Determination of Reverse Turns in the $^{1}H\{^{15}N\}$SBC-NOE Spectrum. In general, the identification of turns relies on the observation of short stretches of characteristic $d_{\alpha N}(i,i+1)$ and $d_{NN}(i,i+1)$ NOE connectivities, along with $d_{\alpha N}(i,i+2)$ and $d_{NN}(i,i+2)$ NOE's between those amino acid residues involved in turn formation (Wüthrich et al., 1984; Wagner et al., 1986). In the $^{1}H\{^{15}N\}$SBC-NOE spectrum a reverse turn is characterized by only one or two steps in the ^{15}N-assisted d_{NN} connectivity region and by several connectivities in the ^{15}N-assisted $d_{\alpha N}$ connectivity region. The latter starts with an NOE relay

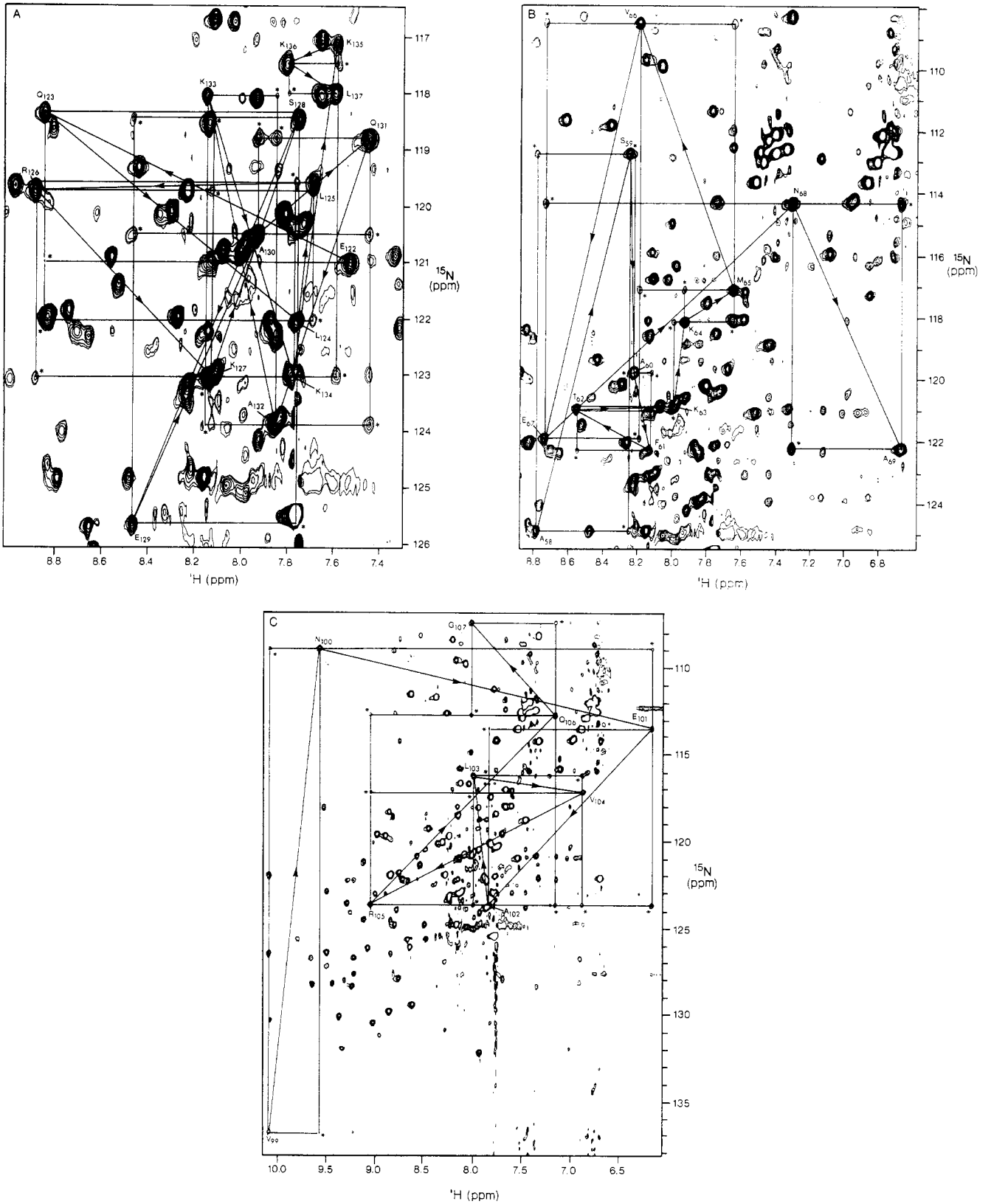

FIGURE 10: Assignments of cross peaks diagnostic of α-helical segments in the $^{1}H^{N}$–^{15}N connectivity region of the 600-MHz $^{1}H\{^{15}N\}$SBC-NOE spectrum of ^{15}N-labeled staphylococcal nuclease ternary complex ([95% ul ^{15}N]H124L-TC). The $^{1}H^{N}_{i}$–$^{15}N_{i+1}$ and $^{1}H^{N}_{i+1}$–$^{15}N_{i}$ NOE relay cross peaks are indicated by asterisks. (A) ^{15}N-Assisted d_{NN} sequential NOE connectivities assigned to Glu^{122}–Leu^{137}. (B) ^{15}N-Assisted d_{NN} sequential NOE connectivities assigned to Ala^{58}–Ala^{69}. (C) ^{15}N-Assisted d_{NN} sequential NOE connectivities assigned to Val^{99}–Gly^{107}.

cross peak connecting $^{1}H^{\alpha}_{i}$ and $^{1}H^{N}_{i}$ at the $^{15}N_{i}$ chemical shift and proceeds through an NOE relay cross peak connecting $^{1}H^{\alpha}_{i}$ and $^{1}H^{N}_{i+1}$ at the $^{15}N_{i+1}$ chemical shift to an NOE relay cross peak between $^{1}H^{\alpha}_{i+1}$ and $^{1}H^{N}_{i+1}$ at the $^{15}N_{i+1}$ chemical shift. Because the residual water peak lies in the $^{1}H^{\alpha}$–^{15}N chemical shift region, the search for $d_{\alpha N}$ NOE relay cross peaks is not always successful. Thus the identification of reverse turns in the $^{1}H^{\alpha}$–^{15}N region can be difficult.

The solution structure of staphylococcal nuclease H124L contains several turns. A search of the $^{1}H^{N}$–^{15}N and $^{1}H^{\alpha}$–^{15}N regions revealed two short d_{NN} sequential stretches and one short $d_{\alpha N}$ sequential connectivity. The first short d_{NN} se-

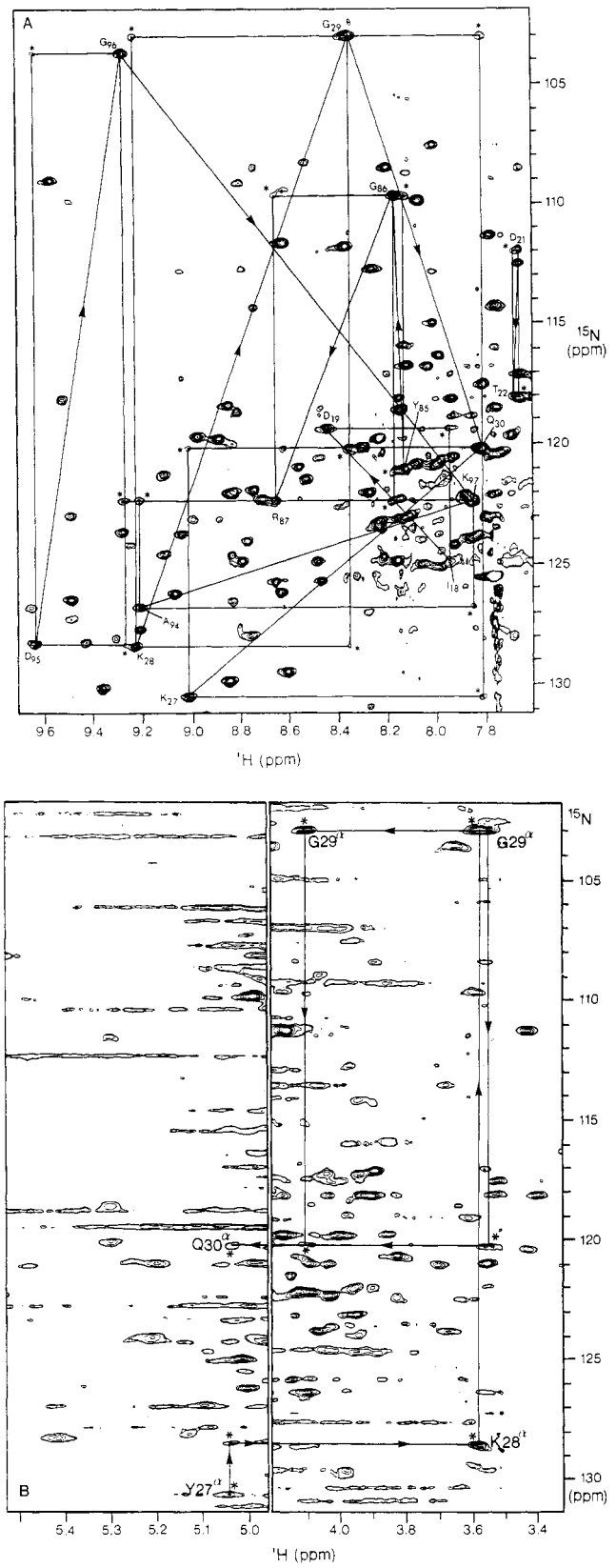

FIGURE 11: Portions of the $^1H^N$–^{15}N connectivity region of the 600-MHz $^1H\{^{15}N\}$SBC-NOE spectrum of ^{15}N-labeled staphylococcal nuclease ternary complex ([95% ul ^{15}N]H124L-TC). (A) ^{15}N-Assisted d_{NN} sequential NOE connectivities that arise from reverse turns. (B) A short ^{15}N-assited $d_{\alpha N}$ sequential NOE walk within a turn.

quential walk was assigned to a segment of three residues as shown in Figure 11A. No related sequential $d_{\alpha N}$ connectivities were found. The amide proton chemical shifts of this segment assign it to Asn^{95}–Lys^{97}, a short segment previously identified as a reverse turn (Wang et al., 1990). The second short d_{NN} walk (Figure 11A) involves three amino acid residues. On the basis of $^1H^N$ chemical shifts, this segment is assigned to Lys^{28}–Gln^{30}. The d_{NN} connectivities between Ala^{94} and Lys^{97} and between Tyr^{27} and Gln^{30} within this turn were also observed. As shown in Figure 11B, evidence was found in the $^1H^\alpha$–^{15}N region for $d_{\alpha N}$ sequential connectivities that define a four-residue turn, Tyr^{27}–Gln^{30}.

The ^{15}N-assisted d_{NN} NOE connectivities between Ile^{18} and Asp^{19} and between Asp^{21} and Thr^{22} (Figure 11A) confirm that these residues form a reverse turn within an antiparallel β-sheet (Wang et al., 1990). The three-residue segment, Tyr^{85}-Gly^{86}-Arg^{87}, which constitutes one of the turns in the large loop of the nuclease backbone presents a short stretch of ^{15}N-assisted d_{NN} NOE connectivities (Figure 11A). The $^1H^N$ chemical shifts of Tyr^{85} (8.15 ppm) and Gly^{86} (8.18 ppm) are so close that the d_{NN} cross peaks between them are located in the NOESY diagonal. As shown in Figure 11A, differences in the ^{15}N chemical shifts of these residues makes them easy to distinguish in $^1H\{^{15}N\}$ experiments. In the $^1H\{^1H\}$NOESY (H_2O) spectrum, the Arg^{87} $^1H^N$ has the same chemical shift as the Lys^{84} $^1H^N$. Thus, the d_{NN} sequential assignment from Gly^{86} and Arg^{87} is ambiguous. The ^{15}N-assisted d_{NN} connectivity between these two residues removes this uncertainty. The ^{15}N chemical shifts of the amino acid residues within the identified turns are listed in Table I.

Recognition of Interstrand NOE Connectivity Patterns Corresponding to Antiparallel β-Sheet in $^1H\{^{13}C\}$SBC-NOE Spectra. Staphylococcal nuclease H124L has a high content of antiparallel β-sheet. Characteristic NMR features of antiparallel β-sheet are strong $d_{\alpha N}(i,i+1)$ NOE connectivities and interstrand $d_{\alpha\alpha}(i,j)$ NOE connectivities. In addition, long-range d_{NN} and $d_{\alpha N}$ NOE connectivities between two adjacent strands also can be observed (Wüthrich et al., 1984; Wagner et al., 1986; Englander et al., 1987). $^1H\{^{13}C\}$SBC-NOE data can provide an efficient approach in some cases to analyzing $d_{\alpha\alpha}(i,j)$ connectivities. The results can be very useful in removing uncertainties in NOESY data interpretation.

The region of the $^1H\{^{13}C\}$SBC-NOE spectrum shown in Figure 6B contains two types of cross peaks: direct $^1H^\alpha$–$^{13}C^\alpha$ cross peaks (along with direct $^1H^\beta$–$^{13}C^\beta$ cross peaks from threonine and serine) and NOE relay cross peaks, $^1H^\alpha_i$–$^{13}C^\alpha_j$ and $^1H^\alpha_j$–$^{13}C^\alpha_i$. The $d_{\alpha\alpha}(i,j)$ NOE relay cross peaks are indicated by asterisks. Because the ^{13}C chemical shift dispersion is much larger than that of the proton, such data are valuable in identifying NOE's between protons that have similar chemical shifts.

Several pairs of NOE relay cross peaks in Figure 6B represent interstrand NOE connectivities. Residues Ala^{12} and Tyr^{27} of H124L-TC have very similar $^1H^\alpha$ chemical shifts (4.99 and 5.03 ppm, respectively), and it would be difficult to detect an NOE between them in a NOESY spectrum. The pair of NOE relay cross peaks that link these two positions (Figure 6B) provides evidence that Ala^{12} and Tyr^{27} are located in opposite strands of an antiparallel β-sheet. Selective ^{13}C labeling of lysine, methionine, and arginine residues permitted the identification of the direct $^1H^\alpha$–$^{13}C^\alpha$ cross peaks of all 23 lysines, 4 methionines, and 5 arginines of the protein (Figure 6A). Interstrand NOE connectivities between the α-protons of Lys^{24} and Thr^{33}, Tyr^{93} and Met^{98}, and Arg^{35} and Thr^{22} were readily identified. Moreover, a $d_{\alpha\alpha}$ NOE relay cross peak between Glu^{75} and Lys^{9} is observed in Figure 6B. In order to determine if this represents an interstrand $d_{\alpha\alpha}$ NOE, a search was conducted for a $d_{\alpha\alpha}$ NOE connectivity between Pro^{11} and Glu^{73}. A pair of strong NOE relay cross peaks was

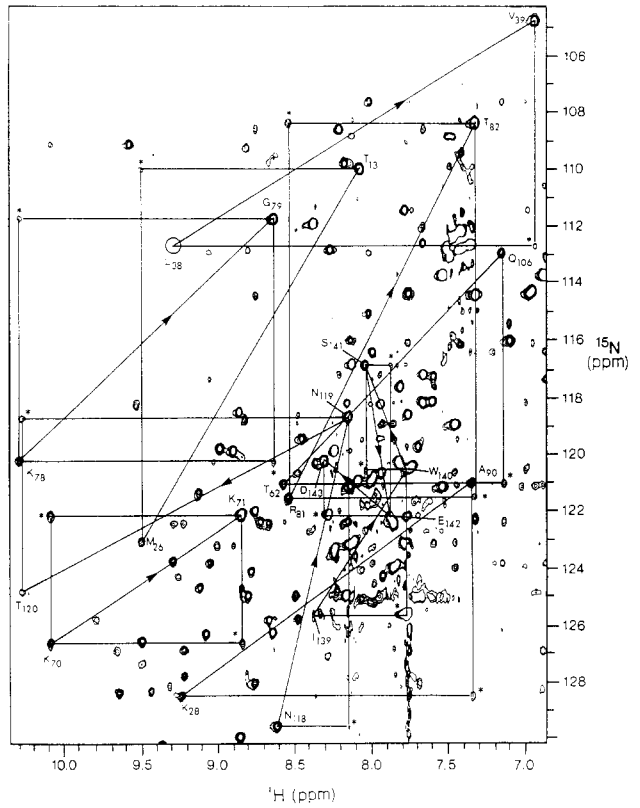

FIGURE 12: Portion of the $^1H^N$–^{15}N connectivity region of the 600-MHz $^1H\{^{15}N\}$SBC-NOE spectrum of ^{15}N-labeled staphylococcal nuclease ternary complex ([95% ul ^{15}N]H124L-TC). Two short ^{15}N-assisted d_{NN} sequential connectivities corresponding to small pieces of helix are indicated by solid lines. The single-step ^{15}N-assisted d_{NN} NOE connectivities indicated in the figure arise from loop and backbone folding. The direct cross peak at Thr^{120} is folded back in from $^1H^N$ = 10.54 ppm.

found to connect the direct cross peaks assigned to Glu^{73} and Pro^{11} (Figure 6B). Since Glu^{75} and Glu^{73} are located in one strand of the antiparallel β-sheet, Lys^9 and Pro^{11}, which form $d_{\alpha\alpha}$ NOE's with them, should be located in the opposite strand. Moreover, the well-defined interstrand $d_{\alpha\alpha}$ connectivities of Val^{39} and Val^{111}, Thr^{82} and Gly^{88}, Ile^{72} and Ala^{94}, Thr^{41} and Ala^{109}, and Ile^{92} and Val^{74} observed in NOESY spectra (Wang et al., 1990) are all identified by NOE relay connectivity networks (solid lines in Figure 6B).

Backbone Conformation from Short Random d_{NN} Connectivities Provided by $^1H\{^{15}N\}$SBC-NOE Data. The NOE relay cross peaks in the amide region of the $^1H\{^{15}N\}$SBC-NOE spectrum should provide the kind of backbone conformational information contained in the $^1H^N$–$^1H^N$ region of the $^1H\{^1H\}$NOESY spectrum. A search of the amide region revealed several pairs of ^{15}N-assisted d_{NN} connectivities consisting of a single step: Lys^{70}–Lys^{71}, Lys^{78}–Gly^{79}, Arg^{81}–Thr^{82}, Lys^{28}–Ala^{90}, and Thr^{62}–Gln^{106} (Figure 12). They provide information on loop and backbone folding (Wang et al., 1990).

Staphylococcal nuclease H124L-TC also contains several small pieces of helix. A further search revealed two short segments of random d_{NN} connectivities (Figure 12). A stretch of five residues was assigned to helix Ile^{139}–Asp^{143} on the basis of the readily identified direct $^1H^N$–^{15}N cross peak of Ser^{141}. A three-residue stretch was assigned to Asn^{118}-Asn^{119}-Thr^{120} on the basis of the direct cross peak of Thr^{120} (Figure 12); these residues form part of a type III reverse turn (Wang et al., 1990).

Conclusions

In this paper we describe sequence-specific assignments of NMR signals from the ternary complex of staphylococcal nuclease (H124L-TC) to ^{13}C and ^{15}N atoms and to ^1H atoms of the side chains. The present assignments were obtained by the combined use $^1H\{^{13}C\}$SBC, $^1H\{^{13}C\}$SBC-HH, $^1H\{^{13}C\}$-SBC-NOE, and $^1H\{^{15}N\}$SBC-NOE experiments. Assignments of ^{13}C spin systems will be completed by carbon–carbon double-quantum correlation spectroscopy ($^{13}C\{^{13}C\}$DQC) (Oh et al., 1988).

Secondary structural elements of the ternary complex were determined by heteronuclear single-bond correlation experiments containing an NOE relay: $^1H\{^{13}C\}$SBC-NOE and $^1H\{^{15}N\}$SBC-NOE. Reverse turns and α-helices were determined by the $^1H\{^{15}N\}$SBC-NOE experiment alone. Antiparallel β-sheet was identified from $^1H\{^{13}C\}$SBC-NOE data. In most cases, the results served to confirm secondary structure determinations based previously on $^1H\{^1H\}$ NOESY data (Wang et al., 1990). In several cases, the heteronuclear 2D data removed ambiguities and uncertainties inherent in the NOESY data.

Acknowledgments

We thank Professor David M. LeMaster for providing insights and materials necessary for the protein production, Professors Julius Adler and Carol A. Gross for supplying amino acid auxotrophs of *E. coli*, Denise Benway for expert assistance in amino acid analysis, Bin Yuan for providing the ^{15}N-labeled leucine sample, and Dr. Dennis A. Torchia for providing copies of manuscripts prior to publication.

References

Alexandrescu, A. T., Mills, D. A., Ulrich, E. L., Chinami, M., & Markley, J. L. (1988) *Biochemistry 27*, 2158–2165.
Bax, A., & Summers, M. F. (1986) *J. Am. Chem. Soc. 108*, 2093–2094.
Cohen, J. S., Feil, M., & Chaiken, I. M. (1970) *Biochim. Biophys. Acta 236*, 468–478.
Englander, S. W., & Wand, A. J. (1987) *Biochemistry 26*, 5953–5958.
Evans, P. A., Dobson, C. M., Kautz, R. A., Hatfull, G., & Fox, R. O. (1987) *Nature 329*, 266–268.
Grissom, C. B., & Markley, J. L. (1989) *Biochemistry 28*, 2116–2124.
Hibler, D. W., Stolowich, N. J., Reynolds, M. A., & Gerlt, J. A. (1987) *Biochemistry 26*, 6278–6286.
Jardetzky, O., Markley, J. L., Williams, M. N., Thielmann, H., & Arata, Y. (1972) *Cold Spring Harbor Symp. Quant. Biol. 36*, 257–261.
LeMaster, D. M., & Richards, F. (1982) *Anal. Biochem. 122*, 238–247.
Maniatis, T., Fritsch, E. F., & Sambrook, J. (1982) *Molecular Cloning. A Laboratory Manual*, Cold Spring Harbor Laboratory, Cold Spring Harbor, NY.
Markley, J. L., Putter, I., & Jardetzky, O. (1968) *Science 161*, 1249–1251.
Oh, B.-H., Westler, W. M., Darba, P., & Markley, J. L. (1988) *Science 240*, 908–911.
Oh, B.-H., Westler, W. M., & Markley, J. L. (1989) *J. Am. Chem. Soc. 111*, 3083–3085.
Shon, K., & Opella, S. J. (1989) *J. Magn. Reson. 82*, 193–197.
Shortle, D. (1986) *J. Cell. Biochem. 30*, 281–289.
Sklenar, V., & Bax, A. (1987) *J. Magn. Reson. 71*, 379–383.
Studier, F. W., & Moffatt, B. A. (1986) *J. Mol. Biol. 189*, 113–130.
Taniuchi, H., Anfinsen, C. B., & Sodja, A. (1967) *Proc. Natl. Acad. Sci. U.S.A. 58*, 1235–1242.

Torchia, D. A., Sparks, S. W., & Bax, A. (1989) *Biochemistry 28*, 5509–5524.
Tucker, D. W., Hazen, E. E., Jr., & Cotten, F. A. (1978) *Mol. Cell. Biochem. 22*, 67–77.
Tucker, D. W., Hazen, E. E., Jr., & Cotten, F. A. (1979) *Mol. Cell. Biochem. 23*, 3–16, 67–86, 131–141.
Wagner, G., Neuhaus, D., Wörgötter, E., Vasak, M., Kagi, J. H. R., & Wüthrich, K. (1986) *J. Mol. Biol. 187*, 131–135.
Wang, J., LeMaster, D. M., & Markley, J. L. (1990) *Biochemistry* (preceding paper in this issue).
Wüthrich, K. (1984) *J. Mol. Biol. 180*, 715–740.
Wüthrich, K. (1986) *NMR of Proteins and Nucleic Acids*, Wiley, New York.

Complex Formation of Peptide Antibiotic Ro09-0198 with Lysophosphatidylethanolamine: ^{1}H NMR Analyses in Dimethyl Sulfoxide Solution†

Kaori Wakamatsu,*,‡,§ Se-Young Choung,‖ Tetsuyuki Kobayashi,‖ Keizo Inoue,‖ Tsutomu Higashijima,‡,⊥ and Tatsuo Miyazawa*,#

Department of Biophysics and Biochemistry, Faculty of Science, and Department of Health Chemistry, Faculty of Pharmaceutical Sciences, University of Tokyo, Hongo, Bunkyo-ku, Tokyo 113, Japan, and Faculty of Engineering, Yokohama National University, Hodogaya-ku, Yokohama 240, Japan

Received May 23, 1989; Revised Manuscript Received August 17, 1989

ABSTRACT: Ro09-0198 is a peptide antibiotic and immunopotentiator produced by *Streptoverticillium griseoverticillatum* which exhibits antitumor and antimicrobial activities. The chemical structure has been determined [Kessler et al. (1988) *Helv. Chim. Acta 71*, 1924–1929; Wakamiya et al. (1988) *Tetrahedron Lett. 37*, 4771–4772]. This peptide specifically interacts with (lyso)phosphatidylethanolamine, causing hemolysis and enhancing permeability in phosphatidylethanolamine-containing vesicles [Choung et al. (1988) *Biochim. Biophys. Acta 940*, 171–179, 180–187]. The highly specific nature of the interaction was studied by two dimensional proton NMR analyses. Proton resonances of the peptide were observed in dimethyl sulfoxide solution in the presence of 1-dodecanoyl-*sn*-glycerophosphoethanolamine. By comparison to the chemical shifts in the absence of lysophosphatidylethanolamine and by analysis of intermolecular cross-peaks in NOESY spectra, amino acid residues involved in the binding with the phospholipid were identified. The ammonium group of the phospholipid interacts with the carboxylate group of β-hydroxyaspartic acid-15 but not with that of the carboxylate terminus. The secondary ammonium group of lysinoalanine-19/6 is probably bound to the phosphate group of the lipid. The peptide does not interact strongly with the fatty acid chain of the lipid. A folded structure of the central part [from Phe^7 to Ala(S)^{14}] of the peptide opens on binding with the phospholipid and accommodates the glycerophosphoethanolamine head group.

Ro09-0198 is a peptide antibiotic and immunopotentiator found in culture fluid of *Streptoverticillium griseoverticillatum* which exhibits antitumor and antimicrovial activity (Takemoto, 1981). Kessler et al. (1987, 1988) determined the chemical structure of the peptide by a combination of chemical methods and a variety of NMR methods. Independently, Wakamiya et al. (1988) determined the peptide structure (including the chirality of amino acid residues) by chemical methods. It is a nonadecapeptide containing various uncommon amino acids, lanthionine, β-methyllanthionine, lysinoalanine, and β-hydroxyaspartic acid, the former three forming intramolecular bridges (Figure 1a).

The amino acid composition of this peptide is quite similar to that of duramycin (Arg^2 is replaced by lysine in duramycin; Shotwell et al., 1958), which suggests similar action mechanisms of these antibiotics. In fact, these peptides have been found to interact specifically with certain lipid components of the cell membrane. Duramycin induces aggregation of lipid vesicles containing phosphatidylethanolamine or monogalactosyldiglyceride (Navaro et al., 1985), while Ro09-0198 induces hemolysis which is blocked by preincubation of the peptide with phosphatidylethanolamine-containing vesicles (Choung et al., 1988a,b). Ro09-0198 is also found to cause leakage of small molecules from vesicles containing phosphatidylethanolamine or lysophosphatidylethanolamine. The interaction of Ro09-0198 with lipids is highly specific, and the structural requirement for the lipid is the presence of the phosphoethanolamine moiety with a free primary amino group and a hydrophobic chain. In addition, the glycerol moiety is required for the permeability increase through the lipid bilayer (Choung et al., 1988a,b).

† This work was supported in part by a Grant-in-Aid for Scientific Research from the Ministry of Education, Science and Culture of Japan.
* Authors to whom correspondence should be addressed.
‡ Faculty of Science, University of Tokyo.
§ Present address: Tsukuba Research Laboratories, Takeda Chemical Industries, Ltd., Wadai, Tsukuba, Ibaraki 300-42, Japan.
‖ Faculty of Pharmaceutical Sciences, University of Tokyo.
⊥ Present address: Department of Pharmacology, Southwestern Graduate School, University of Texas Health Science Center, Dallas, TX 75235.
Faculty of Engineering, Yokohama National University.

0006-2960/90/0429-113$02.50/0